RESEARCH ARTICLE

Molecular Reproduction & Development 82:281–294 (2015)

Redox and Anti-Oxidant State Within Cattle Oocytes Following In Vitro Maturation With Bone Morphogenetic Protein 15 and Follicle Stimulating Hormone

MELANIE L. SUTTON-MCDOWALL,[1,2,3]* MALCOLM PURDEY,[2,3] HANNAH M. BROWN,[1] ANDREW D. ABELL,[2,3] DAVID G. MOTTERSHEAD,[1] PABLO D. CETICA,[4] GABRIEL C. DALVIT,[4] EWA M. GOLDYS,[2,5] ROBERT B. GILCHRIST,[1,7] DAVID K. GARDNER[6], AND JEREMY G. THOMPSON[1,2,3]

[1] Robinson Research Institute, School of Paediatrics and Reproductive Health, The University of Adelaide, Medical School, Adelaide, South Australia, Australia
[2] Australian Research Council Center of Excellence for Nanoscale BioPhotonics, Australia
[3] Institute for Photonics and Advanced Sensing, The University of Adelaide, Adelaide, South Australia, Australia
[4] Institute of Research and Technology on Animal Reproduction, School of Veterinary Sciences, University of Buenos Aires, Buenos Aires, Argentina
[5] MQ BioFocus Research Center, Macquarie University, North Ryde, New South Wales, Australia
[6] Department of Zoology, The University of Melbourne, Parkville, Victoria, Australia
[7] Discipline of Obstetrics and Gynaecology, University of New South Wales, School of Womens and Childrens Health, Sydney, Australia

SUMMARY

The developmental competence of cumulus oocyte complexes (COCs) can be increased during in vitro oocyte maturation with the addition of exogenous oocyte-secreted factors, such as bone morphogenetic protein 15 (BMP15), in combination with hormones. FSH and BMP15, for example, induce different metabolic profiles within COCs—namely, FSH increases glycolysis while BMP15 stimulates FAD and NAD(P)H accumulation within oocytes, without changing the redox ratio. The aim of this study was to investigate if this BMP15-induced NAD(P)H increase was due to de novo NADPH production. Cattle COCs were cultured with FSH and/or recombinant human BMP15, resulting in a significant decrease in glucose-6-phosphate dehydrogenase activity ($P < 0.05$). Inhibition of isocitrate dehydrogenase (IDH) during this process decreased NAD(P)H intensity threefold in BMP15-treated oocytes, suggesting that BMP15 stimulates IDH and NADPH production via the tricarboxylic acid cycle. As NADPH is a reducing agent, reduced glutathione (GSH), H_2O_2, and mitochondrial activity were also measured to assess the general redox status of the oocyte. FSH alone decreased GSH levels whereas the combination of BMP15 and FSH sustained higher levels. Expression of genes encoding glutathione-reducing enzymes were also lower in oocytes cultured in the presence of FSH alone. BMP15 supplementation further promoted mitochondrial localization patterns that are consistent with enhanced developmental competence. Metabolomics revealed significant consumption of glutamine and production of alanine by COCs matured with both FSH and BMP15 compared to the control ($P < 0.05$). Hence, BMP15 supplementation differentially modulates reductive metabolism and mitochondrial localization within the oocyte. In comparison, FSH-stimulation alone decreases the oocytes' ability to regulate cellular stress, and therefore utilizes other mechanisms to improve developmental competence.

Mol. Reprod. Dev. 82: 281–294, 2015.

Received 2 December 2014; Revised 29 January 2015; Accepted 2 February 2015

*Corresponding author:
Medical School South,
Frome Road,
Adelaide, South Australia 5005, Australia.
E-mail: melanie.mcdowall@adelaide.edu.au

Current address of Robert B. Gilchrist is School of Womens & Childrens Health, Discipline of Obstetrics & Gynaecology, University of New South Wales, Sydney 2052, Australia.

Grant sponsor: National Health and Medical Research Council Australia (NHMRC) Project; Grant number: 1008137; Grant sponsor: NHMRC Development; Grant number: 1017484; Grant sponsor: NHMRC Fellowship; Grant number: 627007; Grant sponsor: Australian Research Council Centre of Excellence for Nanoscale BioPhotonics; Grant number: CE140100003

Published online 26 February 2015 in Wiley Online Library (wileyonlinelibrary.com).
DOI 10.1002/mrd.22470

INTRODUCTION

The oocyte and its surrounding specialized somatic cells (cumulus cells)—together referred to as the cumulus-oocyte complex (COC)—share a symbiotic relationship during the final stages of oocyte development and immediately prior to ovulation (Albertini et al., 2001; Matzuk et al., 2002). Bi-directional communication between these cell populations, which is facilitated by paracrine and gap junction communication, is critical for the oocyte to achieve developmental competence—the ability to undergo successful fertilization and embryo development (Larsen and Wert 1988; Buccione et al., 1990a; Albertini et al., 2001). Cumulus cells provide the oocyte with nutrients and factors essential for maturation (Sutton et al., 2003; Krisher 2013). In return, the oocyte secretes growth factors (oocyte-secreted factors) that facilitate the differentiation of cumulus cells from other somatic ovarian cells (Li et al., 2000); increases mucification and proliferation (Buccione et al., 1990a; Salustri et al., 1990a, 1990b); increases steriodogenesis (Vanderhyden and Macdonald, 1998); and prevents apoptosis (Hussein et al., 2005). Oocyte-secreted factors include growth differentiation factor 9 (GDF9) and bone morphogenetic protein 15 (BMP15), which are both members of the transforming growth factor β superfamily (Su et al., 2004). BMP15 in particular is a potent promoter of oocyte developmental competence in large, mono-ovular species such as cattle (Hussein et al., 2006; Crawford and McNatty, 2012).

We previously reported that recombinant human BMP15 and follicle stimulating hormone (FSH), a potent stimulator of COC metabolism and a common media additive used during in vitro oocyte maturation (IVM), significantly increase bovine oocyte developmental competence when supplemented together (as indicated by increased on-time blastocyst yield per cleaved embryos: $28.4 \pm 7.4\%$ without either versus $51.5 \pm 5.4\%$ with both, $P < 0.05$). Individually, each factor results in similar blastocyst yields ($44.4 \pm 3.9\%$ with FSH versus $41 \pm 2.9\%$ with BMP15, $P > 0.05$), but appears to stimulate different metabolic activities within COCs (Sutton-McDowall et al., 2012). FSH stimulates glucose metabolism in cumulus cells via glycolysis and the hexosamine biosynthetic pathway, as indicated by increased lactate production and mucification that leads to cumulus expansion, whereas BMP15 stimulates oxidative phosphorylation (as measured by FAD autofluorescence) and increased NAD(P)H levels within oocytes. Yet, the cell-specific impact of both FSH and BMP15 on oocyte metabolism is mediated through cumulus cells, as the oocyte itself exhibits low levels of glycolytic activity and increases in intra-oocyte FAD and NAD(P)H levels are only detected in cumulus-enclosed oocytes (Sutton-McDowall et al., 2012).

Quantities of FAD, the oxidized co-factor of $FADH_2$ within complex II of the mitochondrial respiratory chain, and NAD(P)H, representing both the reduced NADH and NADPH co-factors that are involved in numerous metabolic pathways, are often used to assess the redox status of cells (Mayevsky and Chance, 1982; Skala and Ramanujam, 2010). NADH is a co-factor for several metabolic enzymes, such as cytoplasmic lactate dehydrogenase, and is a proton donor within complex I of the mitochondrial respiratory chain, where it is oxidized to NAD^+. NADPH is a co-factor for several enzymes, including glucose-6-phosphate dehydrogenase (G6PDH) during glucose metabolism through the cytoplasmic pentose phosphate pathway and isocitrate dehydrogenase (IDH) in the mitochondrial tricarboxylic acid (TCA) cycle. Intracellular NADH and NADPH levels can be measured by their autofluorescence, albeit they are indistinguishable in somatic cells; however, the majority of NAD(P)H auto-fluorescence represents NADH (Chance et al., 1979). As BMP15 stimulates oxidative phosphorylation over glycolysis in COCs, an increased redox ratio (FAD:NAD(P)H) was predicted, but not observed (Sutton-McDowall et al., 2012), suggesting instead that BMP15 could be elevating intra-oocyte NADPH levels.

While the oocyte itself has a low capacity for glucose uptake and metabolism (Sutton-McDowall et al., 2010), the pentose phosphate pathway is thought to be important for oocyte maturation based on the provision of substrates for de novo nucleic acid synthesis, which generates NADPH in oocytes (Downs et al., 1998). This model has recently been challenged by the demonstration that IDH, of the TCA cycle, supplies the majority of NADPH within mouse oocytes (Dumollard et al., 2007b). Furthermore, only NADP-dependent IDH activity is detected in bovine cumulus cells and oocytes (Cetica et al., 2003).

Regardless of the source, NADPH plays an important role in preventing the accumulation of overt levels of reactive oxygen species (ROS) within the oocyte. Thiol compounds such as glutathione are innate antioxidants that donate protons to convert hydrogen peroxide (H_2O_2) to water. Oxidised glutathione (GSSG) is reduced (GSH) by glutathione reductase (GSR) and glutathione S-transferase (GSTA), which requires NADPH as a co-factor. GSH is important to cellular health. In regards to the oocyte, acquisition of higher GSH levels during oocyte maturation is associated with improved developmental competence (Takahashi et al., 1993; de Matos et al., 1995; Sanchez et al., 2013).

The aim of this study was to investigate the differential metabolic profiles of cattle COCs exposed to FSH and BMP15. In particular, we investigated the source of increased NAD(P)H levels within the oocyte following stimulation by BMP15, and the consequences of elevated NAD(P)H levels on intra-oocyte levels of GSH, mitochondrial activity/localization, and ROS levels.

Abbreviations: BCB, brilliant cresyl blue; BMP15, bone morphogenic protein 15; COC, cumulus-oocyte complex; FSH, follicle stimulating hormone; H_2O_2, hydrogen peroxide; IDH, isocitrate dehydrogenase; IVM, in vitro oocyte maturation; G6PDH, glucose-6-phosphate dehydrogenase; GPX, glutathione peroxidase; GSH, reduced glutathione; GSR, glutathione reductase; GSS, glutathione synthetase; GSSG, oxidized glutathione; GSTA1, glutathione S-transferase; ROS, reactive oxygen species; MCB, monochlorobimane; PF1, peroxyfluor; TCA, tricarboxylic acld

RESULTS

Intra-Oocyte G6PDH Activity

To determine if G6PDH was the source of BMP15-dependent NAD(P)H accumulation in oocytes, COCs were cultured in the presence of brilliant cresyl blue (BCB), a dye that is metabolized by G6PDH; BCB^- oocytes would be indicative of active G6PDH, and thus could contribute to the accumulation of NADPH. The proportion of BCB^- oocytes after 23 hr of culture did not vary among the control, +FSH, and +FSH +BMP15 treatments (Fig. 1). The proportion of BCB^- oocytes following +BMP15 culture was significantly lower than all the other groups ($90.8 \pm 3.4\%$ versus $62.4 \pm 5.7\%$ in control versus +BMP15, respectively; $P < 0.05$). As BMP15 treatment decreased G6PDH activity within the oocyte, the pentose phosphate pathway is not the primary source of NADPH following BMP15 stimulation.

Intra-Oocyte IDH Activity and NAD(P)H Levels

To determine if the BMP15-dependent increased NAD(P)H levels within the oocyte was due to increased IDH activity from the TCA cycle, cultured COCs were treated with oxalomalate, an inhibitor of IDH. A dose of 1 mM oxalomalate was used since the presence of 5 mM resulted in high levels of background fluorescence in the 405 nm excitation/420−520 nm emission spectrum (Supplementary Figure S1). Autofluorescence (NAD(P)H and FAD) was then measured within the oocyte.

There were no significant differences in oocyte NAD(P)H or FAD autofluorescence intensity between 0 and 1 mM oxalomalate treatments in control conditions lacking BMP15 (Fig. 2). COCs cultured in the presence of BMP15 exhibited significantly higher intra-oocyte NAD(P)H intensity compared to the control groups. In contrast, the NAD(P)H intensity was significantly reduced to control-group levels in oocytes exposed to BMP15 and 1 mM oxalomalate ($P < 0.05$) (Fig. 2A). The significant increase in FAD intensity in the presence of BMP15 ($P < 0.05$) was also reversed in the presence of 1 mM oxalomalate (Fig. 2B). Therefore, oxalomalate treatment reduced the BMP15-mediated increases in NAD(P)H and FAD autofluorescence, suggesting that IDH of the TCA cycle is a major source of NADPH within BMP15-treated oocytes.

Intra-Oocyte GSH, Mitochondrial Activity, and ROS Levels

To determine if the presence of FSH and BMP15 influenced mitochondrial activity and localization, cellular stress, and/or endogenous anti-oxidation protection, treated COCs were labelled after 23 hr of culture with monochlorobimane (MCB) to assess GSH abundance; peroxyfluor 1 (PF1) to evaluate H_2O_2 levels; and Mitotracker Red CMXROS to assess mitochondrial activity. COCs cultured in the presence of FSH alone showed a significant decrease in the mean intensity of intra-oocyte MCB compared to all the other treatment groups ($P < 0.001$) (Fig. 3A,

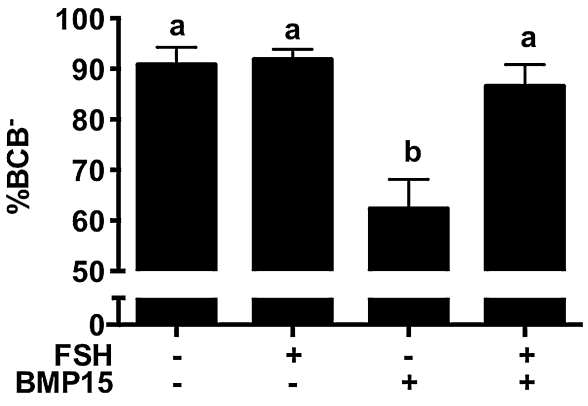

Figure 1. The influence of FSH and BMP15 supplementation during oocyte maturation on G6PDH activity, as determined by BCB staining within the oocyte. Bars represent means + standard error. Different superscripts indicate significant differences (^{ab}, $P < 0.05$).

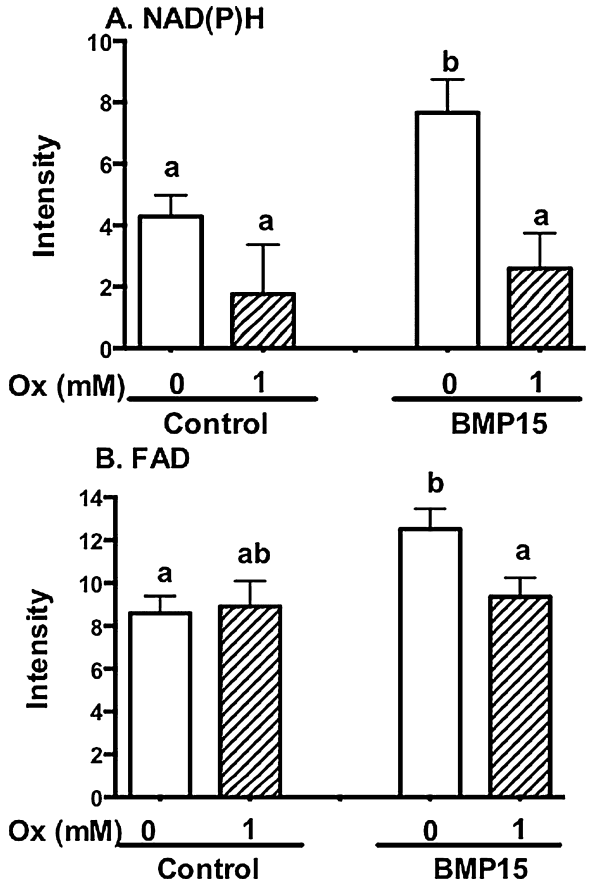

Figure 2. Following 23 hr of culture in the presence or absence of BMP15 (without FSH supplementation), COCs were treated with oxalomalate (Ox), an inhibitor of IDH, followed by measurements of (**A**) NAD(P)H and (**B**) FAD autofluorescence within the oocyte. Bars represent means + standard error. Different superscripts indicate significant differences (^{ab}, $P < 0.05$).

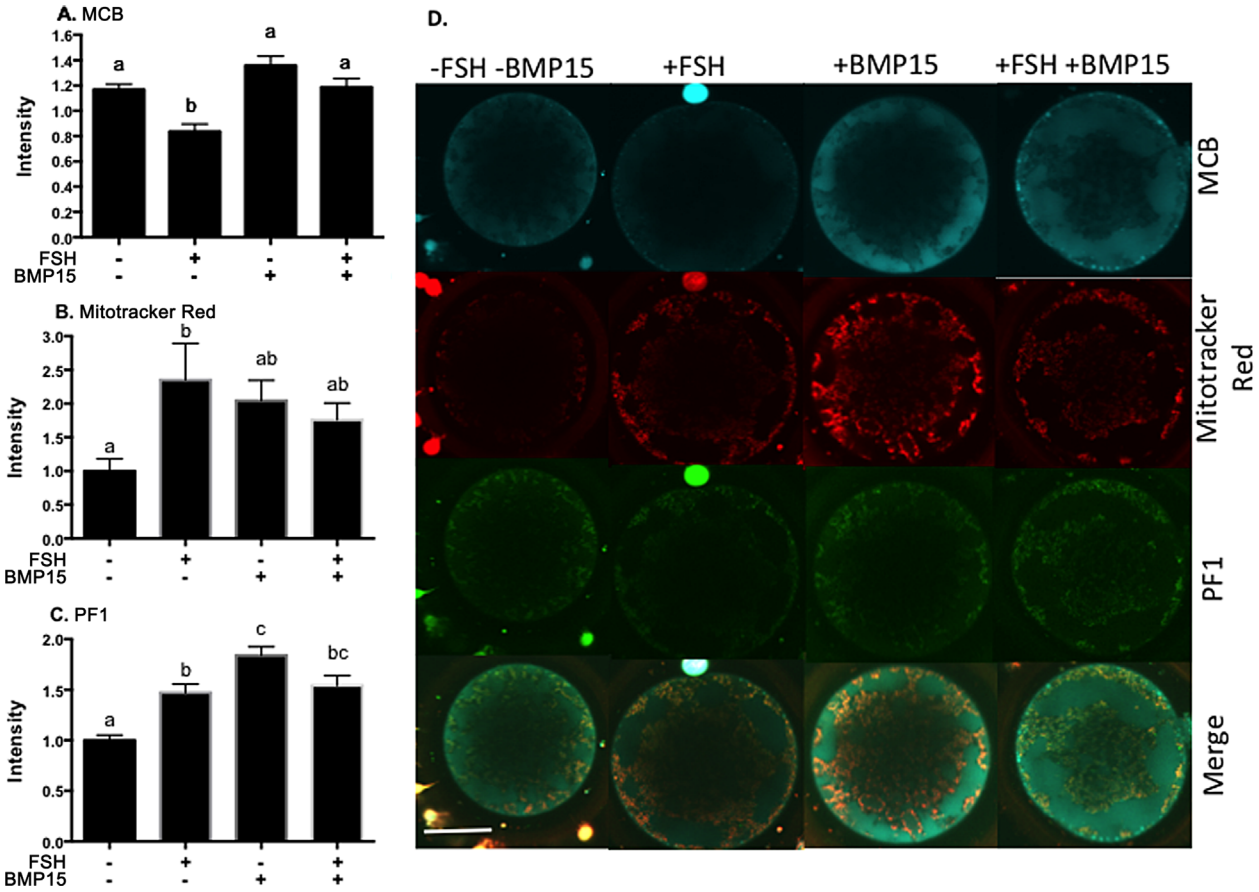

Figure 3. Anti-oxidants, mitochondrial activity, and ROS levels within oocytes matured in the presence of FSH and BMP, as indicated by the mean intensities of (**A**) monochloridebimane (MCB), to assess GSH abundance; (**B**) Mitotracker red CMXROS, to detect active mitochondria; and (**C**) peroxyfluor 1 (PF1), to assess H_2O_2 levels. Bars represent means + standard error. Different superscripts indicate significant differences (^{abc}, $P < 0.05$). (**D**) Representative images of the stained oocytes. Scale bar, 50 μm.

D). In comparison, positive staining for Mitotracker Red (reflecting active mitochondria) was significantly higher within oocytes exposed to FSH during IVM compared to the control group ($P < 0.05$) (Fig. 3B,D). BMP15 or FSH alone significantly increased PF1 levels compared to the control but not the +FSH +BMP15 group (Fig. 3C,D).

To resolve if BMP15 and FSH supplementation during IVM influenced the localization of GSH, H_2O_2, and active mitochondria within the oocyte, image texture analyses were performed with the help of gray-level co-occurrence matrices, which measure levels of roughness or unevenness. Higher co-occurrence matrix values correspond to less uniformity of positive staining in an oocyte. Similar patterns of localization were seen for the angular secondary moment (the texture of the whole oocyte) (Fig. 4), contrast (sub-cellular/organelle texture), and correlation (relationships between neighbouring pixels) (see Supplementary Figure S2). There were no significant differences in the texture patterns of MCB-positive staining (representing GSH) across treatments, likely because of the large variation in patterns seen among all groups ($P > 0.05$) (Fig. 4A). In contrast, BMP15 supplementation resulted in significantly lower texture values, e.g., smoother patterns of positive signal, for PF1 (representing H_2O_2) and Mitotracker Red localization (main effect of BMP15 on Mitotracker Red, $P = 0.005$, and PF1, $P = 0.003$). BMP15 supplementation further resulted in more consistent texture-feature values for both PF1 and Mitotracker Red staining compared to the control group, as indicated by their smaller error bars compared to the control (Fig. 4B–C).

In summary, FSH stimulation reduced levels of GSH-positive staining within oocytes and increased mitochondrial activity and production of H_2O_2 while BMP15 elevated ROS levels in oocytes, regardless of the presence or absence of FSH. BMP15 treatment also promoted a more uniform localization pattern of mitochondria.

Gene Expression Within the Oocyte and Cumulus Vestment

The gene expression of key enzymes involved in glutathione synthesis and cycling—such as glutathione

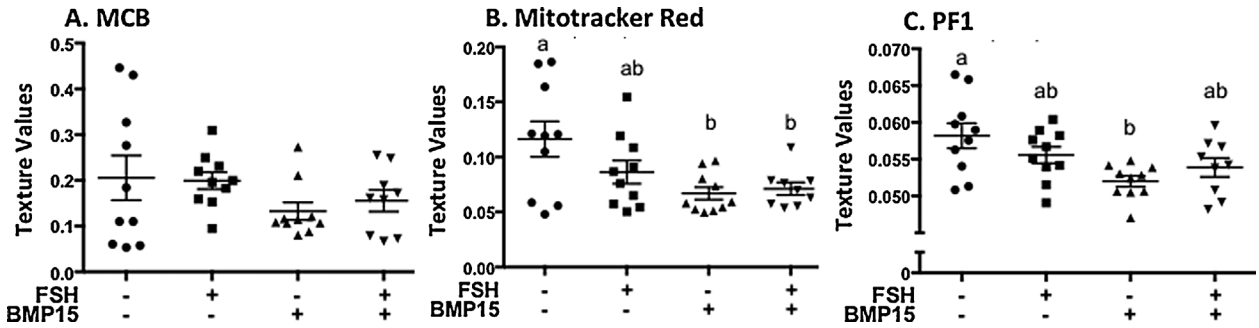

Figure 4. Textural angular-secondary-moment analyses of anti-oxidants, mitochondrial activity, and ROS levels within oocytes matured in the presence of FSH and BMP, as indicated by the values for (**A**) MCB, (**B**) Mitotracker red CMXROS, and (**C**) PF1. Data points indicate individual oocytes; bars represent means ± standard error. Different superscripts indicate significant differences (^{ab}, $P < 0.05$).

biosynthesis (*GSS*), reduction (*GSR, GSTA1*), and oxidation (*GPX1, GPX4*)—were measured in cumulus cells (CC) and COC-derived denuded oocytes (CDO) following 23 hr of maturation in the presence or absence of BMP15 and FSH. In both cumulus cells and denuded oocytes, there were no differences between treatments in regards to the expression of glutathione synthesising (*GSS*) (Fig. 5A–B) and oxidising enzymes (*GPX1* and *GPX4*) (Fig. 5G–N). mRNA expression of *GSR* and *GSTA1*, enzymes involved in the reduction of glutathione, were also similar within the denuded oocyte. FSH supplementation significantly reduced gene expression compared to the control group, regardless of the presence or absence of BMP15 ($P < 0.05$) (Fig. 5D,F). In contrast, *GSTA1* was differentially expressed in cumulus cells, with significantly higher levels in +FSH compared to +BMP15—the opposite of what was seen in denuded oocytes ($P < 0.05$) (Fig. 5E). Therefore, while FSH and BMP15 did not affect the expression of genes involved in glutathione synthesis and oxidation, FSH treatment did significantly influenced glutathione cycling by decreasing the expression of enzymes involved in the reduction of glutathione.

Amino Acid Turnover by Intact Cumulus Oocyte Complexes

Amino acid turnover was measured in conditioned media isolated from the final 4 hr of maturation to determine the metabolic effects of FSH and BMP15 on individual COCs. There were no significant differences in the turnover of total, essential, and nonessential amino acids among treatments (Table 1). Isoleucine, serine, and glutamine were the only amino acids from the media that were consumed by COCs; all other measured amino acids were produced de novo by COCs (Fig. 6). Significant differences in glutamine turnover were observed, with the control group (−FSH −BMP15) producing glutamine as opposed to its consumption in the other treatment groups (−FSH −BMP15, 16.4 ± 23.4, versus +FSH +BMP15, −75.0 ± 16.5 pmol/COC/h) ($P < 0.05$) (Fig. 6). Alanine turnover was also greater than twofold higher in the +FSH and +FSH +BMP15 groups compared to the control group (main effect of FSH, $P < 0.05$) (Fig 6).

DISCUSSION

The addition of native oocyte-secreted factors to oocyte maturation media, either by co-culturing with denuded oocytes or addition of recombinant factors, improves oocyte developmental competence, on-time embryo development rates, and fetal survival post-embryo transfer (Hussein et al., 2006, 2011; Yeo et al., 2008; Sudiman et al., 2014). This simple process appears to help overcome a deficiency in endogenous oocyte-secreted factor production during IVM (Mester et al., 2014). We previously demonstrated that the addition of recombinant, pro-mature BMP15 results in an altered metabolic profile in COCs exposed to FSH, a widely used IVM-media additive that is known to stimulate COC metabolism and oocyte developmental competence (Sutton-McDowall et al., 2012). COCs cultured with BMP15 alone demonstrate a preference for oxidative metabolism, with less glucose metabolized via glycolysis and significant increases in intra-oocyte FAD (Fig. 7). Increased levels of NAD(P)H within the oocyte are also seen, even though the redox ratio among groups is not altered. Therefore, this study investigated the source of the BMP15-dependent increased NAD(P)H levels as well as how this increase may be contributing to improved oocyte health, e.g. via mitochondrial activity and/or the ability to deal with cellular stress.

We hypothesized that the increase in oocyte NAD(P)H could be attributed to increased NADPH production. Indeed, numerous studies have suggested that a major source of NADPH production within the oocyte is through the oxidative arm of the pentose phosphate pathway, specifically via the glucose metabolic actiivty of G6PDH (Downs et al., 1998; Urner and Sakkas, 2005). BCB is metabolized by G6PDH, and has been used to predict the developmental competence of immature oocytes prior to IVM—e.g., low BCB retention indicates active G6PDH, and thus more viable oocytes (Roca et al., 1998; Alm et al.,

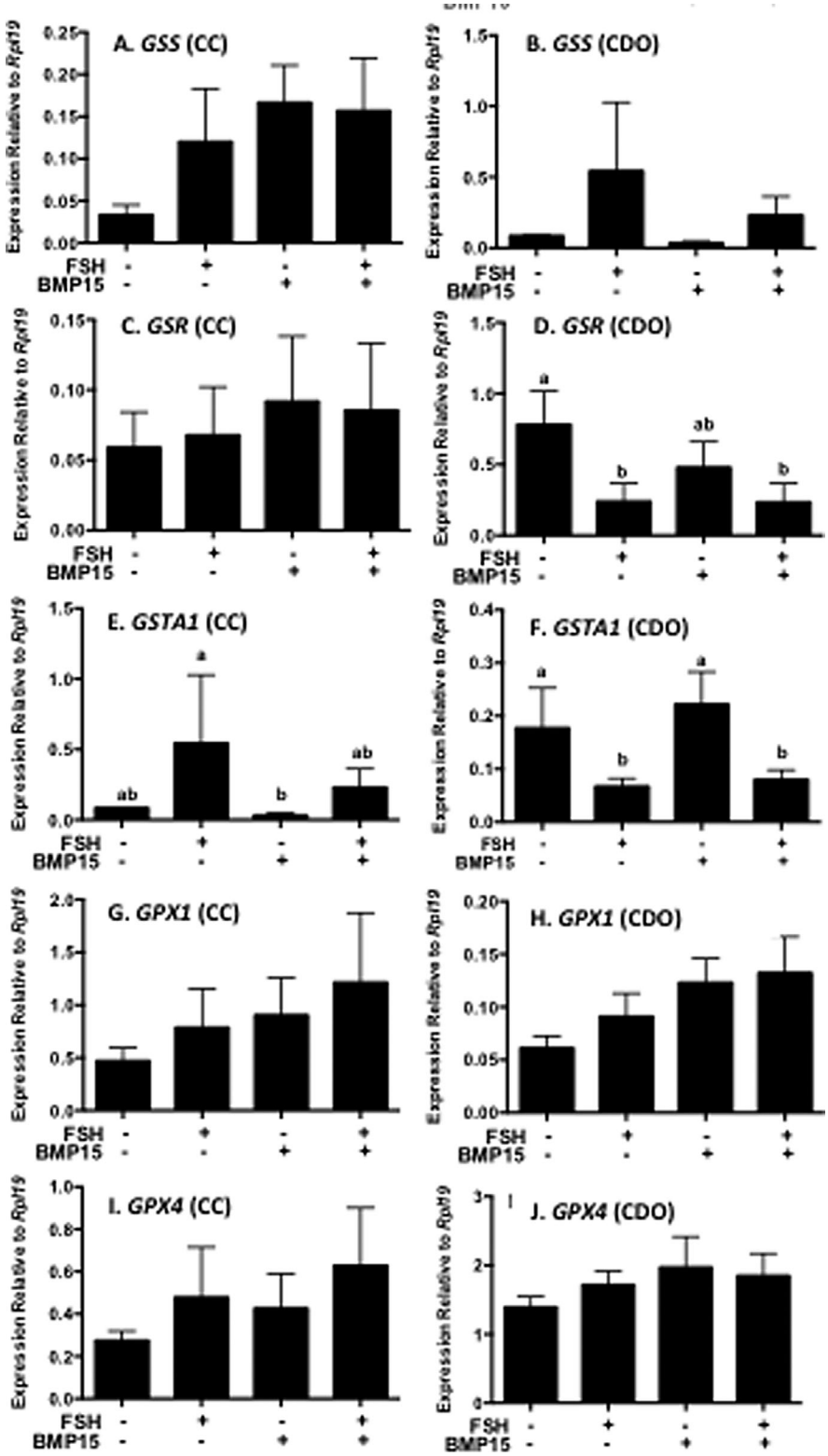

Figure 5. mRNA expression of enzymes involved in NADPH metabolism and glutathione recycling. Intact COCs were cultured in the presence or absence of BMP15 and FSH, and separated into COC-derived oocyte (CDO) and cumulus cells (CC). Bars represent means + standard error. Different superscripts indicate significant differences (^{ab}, $P < 0.05$).

TABLE 1. Total Amino Acid, Essential, and Non-Essential Amino Acid Turn Over by COCs Following Culture in the Presence or Absence of FSH and BMP15

		pmol/COC/h		
FSH	BMP15	Total	Essential	Non-essential
−	−	10.6 ± 2.2	2.56 ± 2.88	30.1 ± 4.1
+	−	11.8 ± 3.2	1.27 ± 2.87	23.8 ± 4.3
−	+	12.9 ± 3.2	−0.22 ± 3.02	17.4 ± 4.2
+	+	16.3 ± 3.0	4.67 ± 2.87	24.2 ± 3.6

Values represent means ± standard error. Negative values represent consumption and positive values represent production.

2005; Bhojwani et al., 2007). In our studies, BMP15 supplementation during COC maturation resulted in fewer BCB^- oocytes, suggesting lower G6PDH and oxidative pentose phosphate pathway activity. In contrast, inhibiting TCA-cycle IDH activity with oxalomalate reduced the BMP15-dependent elevation in NAD(P)H autofluorescence, suggesting that a significant source of intra-oocyte NADPH is the TCA cycle within the oocyte itself. This observation is supported by a report from Dumollard and colleagues, who proposed that TCA-cycle activity, especially that of IDH, contributes significantly to the intracellular redox potential in mouse oocytes (Dumollard et al., 2007b).

A major role of NADPH is the recycling of GSSG to GSH, allowing a cell to respond to oxidative stresses such as H_2O_2 derived from oxidative phosphorylation within the mitochondria. FSH stimulation alone reduced the intensity of MCB staining within the oocyte, implying lower intra-oocyte levels of GSH, whereas additional BMP15 supplementation (+FSH +BMP15) restored MCB intensity. This response is consistent with the reduced transcript levels encoding enzymes involved in the reduction of GSSG to GSH, namely *GSR* and *GSTA1*, within the oocyte following FSH stimulation. Together, these data provide a direct link between FSH stimulation and an oocytes impaired capacity to regulate H_2O_2 levels through glutathione recycling. The increase in blastocyst development following IVM in the presence of both FSH and BMP15, observed in our previous study

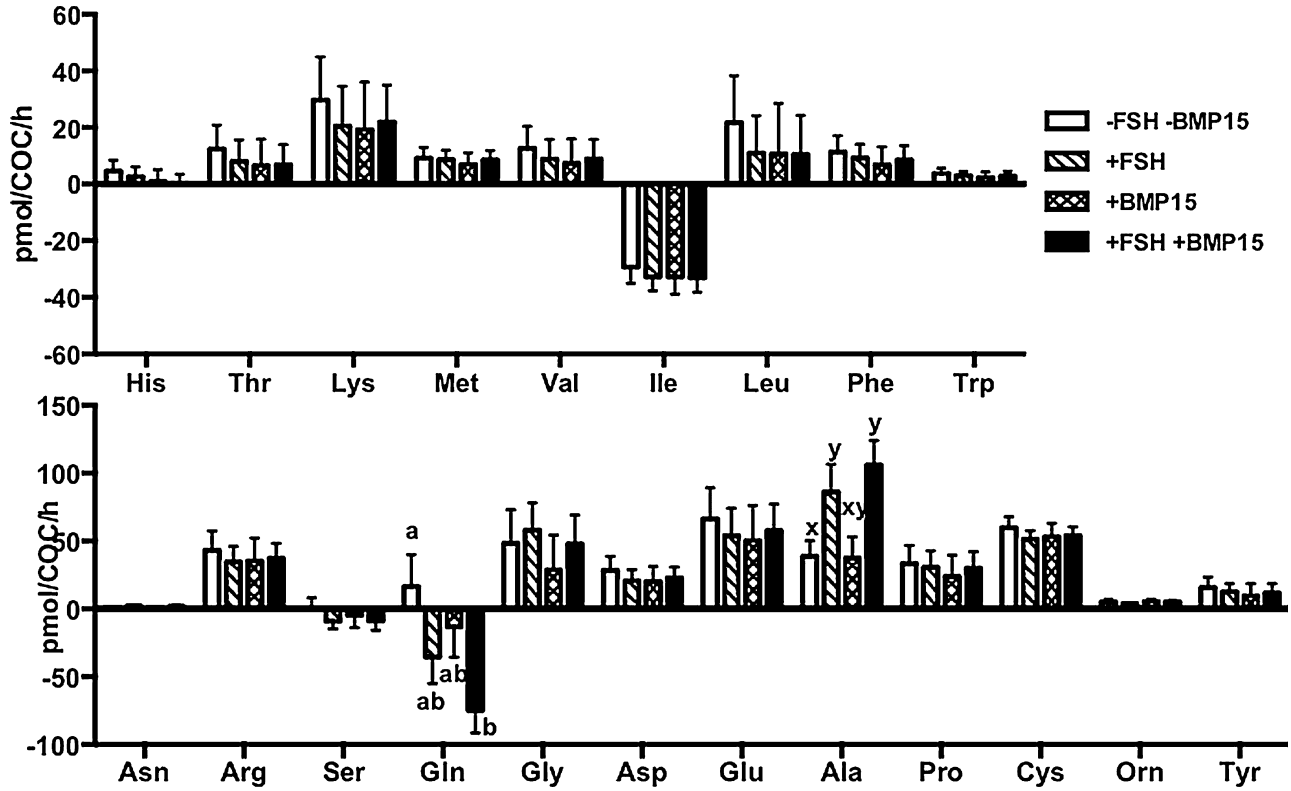

Figure 6. Amino acid turnover by intact COCs cultured in the presence and absence of FSH and BMP15. Bars represent means + standard error. Different superscripts indicate significant differences (^{abxy}, $P < 0.05$).

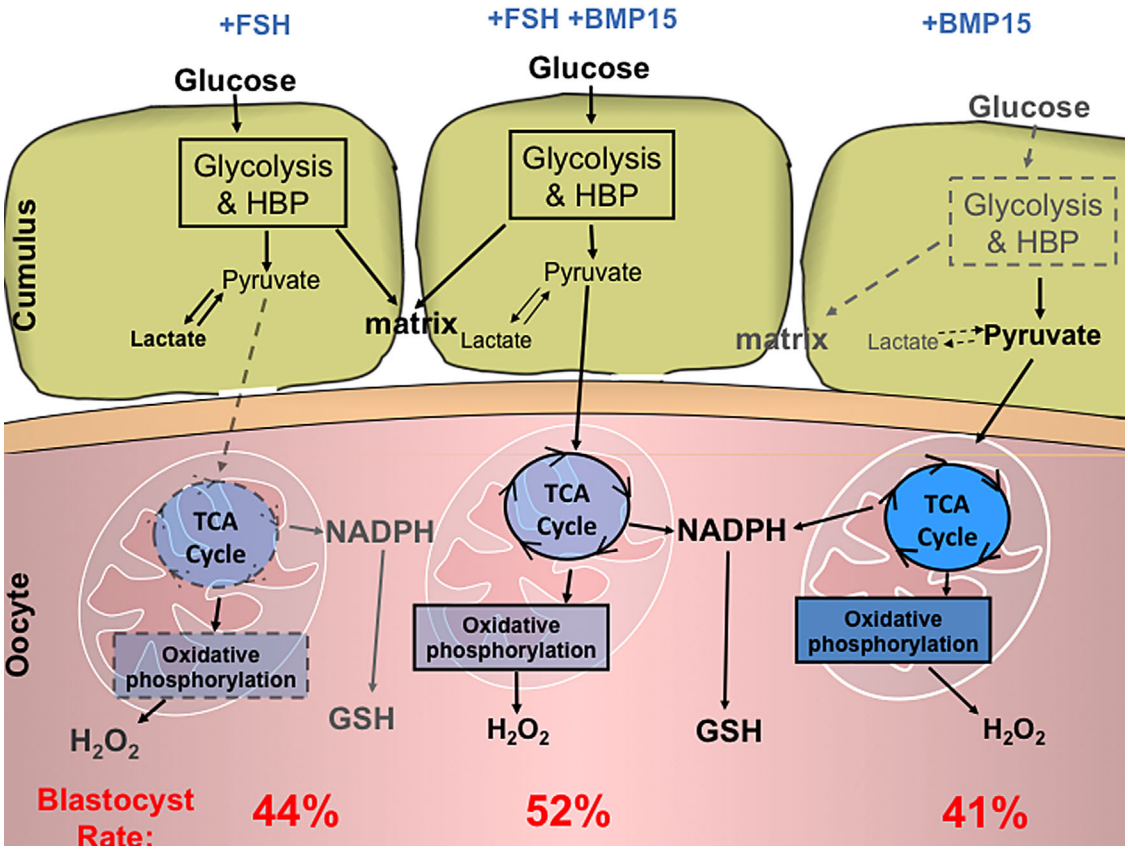

Figure 7. Summary of the changes in metabolism within cumulus cells and oocytes treated with FSH and BMP15. Previous studies demonstrated that the presence of both FSH and BMP15 during IVM significantly increased blastocyst development rates (total blastocysts from cleaved) to 52% compared to 28% without either factor (Sutton-McDowall et al., 2012). Despite similar blastocyst development rates, when FSH and BMP15 were added separately during IVM (44% from +FSH; 41% from +BMP15), different metabolic profiles were observed in the COCs. The presence of FSH alone induces higher levels of glucose metabolism within cumulus cells via glycolysis and the hexosamine biosynthetic pathway (HBP), resulting in the formation of more extracellular matrix. Conversely, the presence of BMP15 alone promotes higher FAD and NADPH/NADH levels within the oocyte. In the current study, BMP15 induced NADPH production via the TCA cycle. Furthermore, mitochondrial localization is more uniform in oocytes treated with BMP15. FSH stimulation reduces GSH levels as well as the transcript abundance of enzymes involved in glutathione reduction, compromising the ability of oocytes to recycle glutathione in response to increased H_2O_2 production from increased mitochondrial activity. BMP15 treatment also resulted in increased H_2O_2 production, but higher levels of GSH, NADPH, and improved mitochondrial localization could counteract this peroxide production.

(Sutton-McDowall et al., 2012), may therefore be attributed to the BMP15-induced increases in NADPH that help sustain GSH levels.

The influence of BMP15 supplementation on oocyte and cumulus-cell metabolism appears to depend on which hormones and growth factors it is co-supplemented with. The metabolism of oocytectomized complexes (intact COCs, in which the ooplasm has been surgically removed), for example, did not differ from intact COCs or oocytectomized complexes co-cultured with denuded oocytes (Sutton et al., 2003)—most likely due to FSH masking the stimulatory effects of BMP15 and other oocyte-secreted factors. Supplementation with the EGF-like peptide amphiregulin plus BMP15 further increased oocyte FAD and NAD(P)H (Sugimura et al., 2014), as opposed to the depression seen with FSH-plus-BMP15 co-stimulation (Sutton-McDowall et al., 2012).

FSH is widely used as a supplement in cattle IVM systems because it can stimulate maturation and other cellular activities, including glucose metabolism (Sutton-McDowall et al., 2010). Yet the drawbacks of FSH are becoming increasingly evident, including its ability to increase cellular stress, as reported here; indeed, alternative hormones and growth factors should be explored. For example, EGF-like peptides improve the developmental competence of oocytes by prolonging gap-junction communication between the oocyte and cumulus cells (Sugimura et al., 2014) and by stimulating glucose metabolism and cumulus-cell expansion in mouse COCs (Richani et al., 2014).

Mean fluorescence intensity and the texture of staining (gray-level co-occurrence matrices) provide a more robust metric of oocyte health when used to evaluate MCB, Mitotracker Red, and PF1 staining. Mitochondria synthesis occurs during oocyte development, and the distribution

of this organelle within the oocyte is constantly changing in response to energy-expensive events such as meiotic progression (Van Blerkom, 2009). Mitochondrial activity is also largely influenced by location with the oocyte (Diaz et al., 1999). For example, immature oocytes (germinal-vesicle stage) demonstrate a cortical pattern of mitochondrial localization, whereas mature (metaphase II) oocytes exhibit a more disperse, uniform distribution (Dumollard et al., 2007a); in contrast, clustering or uneven distribution within metaphase-II oocytes is associated with compromised developmental competence (Van Blerkom, 2009). In the current study, BMP15 supplementation resulted in ''smoother'' and more homogenous localization of both Mitotracker Red and PF1 staining within mature oocytes, independent of the presence of FSH. Furthermore, there was less variation in texture within the +BMP15 and +BMP15+FSH treatment groups when compared to non-supplemented controls. Thus, BMP15 supplementation during IVM is likely promoting the uniform distribution of active mitochondria, thereby contributing to improved function and developmental competence.

A unique aspect of this study was the multiplexed use of fluorescence probes in single, live oocytes to investigate cellular metabolism. Traditional enzymatic assays require pooling large numbers of COCs/oocytes to assess the activity of a single enzyme. Here, fluorescent probes were used instead to determine the level and localization of reactive oxygen species, anti-oxidants (specifically H_2O_2 and GSH), and active mitochondria within cultured oocytes. This technique provided profiles of three metabolic outcomes, with positive staining indicating levels of enzymatic activity, localization, and textural patterning within individual, live oocytes. The use of quantitative texture analyses provided additional metrics to interpret the imaging data. Gray-level co-occurrence matrices have been extensively utilised in diagnostic imaging (Castellano et al., 2004) for dermatology (Mittra and Parekh, 2011), liver (Losa and Castelli, 2005), and cancer (Alvarenga et al., 2007). To our knowledge, this is the first study to present the results of such image analyses to investigate patterns of metabolism within oocytes.

Amino acid profiling provides yet another metric to evaluate oocyte competence following IVM, as highlighted by a recent profile comparison of oocytes denuded of their cumulus-cell vestment compared to intact COCs during the final 6 hr of IVM (Hemmings et al., 2012). Cattle oocytes that underwent successful fertilization, cleavage, and developed to the blastocyst stage (on-time embryo development) had lower glutamine uptake and alanine accumulation in conditioned media compared to incompetent oocytes (uncleaved following fertilization) (Hemmings et al., 2012). A recent study also linked alanine and glutamine levels in follicular fluid with developmental competence of oocytes (Matoba et al., 2014). Here, glutamine consumption and alanine production tracked positively with supplement conditions that yielded bovine COCs with improved oocyte developmental competence. Both glutamine and alanine are generally involved in carbohydrate metabolism among different cell types (Schliess et al., 2014; Varone et al., 2014), so their utility as a general marker of metabolic health in oocytes is expected. Both glutamine metabolism and pyruvate oxidation within cattle oocytes significantly increase towards the end of maturation, as measured in denuded oocytes following COC maturation using radiolabelled substrates (Rieger and Loskutoff, 1994; Steeves and Gardner, 1999). Therefore, it seems reasonable to suggest that within treatments impacting oxidative phosphorylation, such as the addition of BMP15, more glutamine is also metabolized within the oocyte. Similarly, alanine production was highest following FSH treatment, regardless of BMP15 supplementation, and associated with high glycolytic activity (Sutton-McDowall et al., 2012).

In conclusion, BMP15 supplementation during bovine-oocyte IVM stimulates NADPH production via IDH and the TCA cycle within the oocyte, rather than G6PDH of the pentose phosphate pathway. BMP15 supplementation also promoted a more homogenous and consistent localization of active mitochondria, indicative of improved developmental competence. FSH reduces GSH—levels within the oocyte, which corresponded with the reduced gene expression of glutathione-reducing enzymes in treated samples. On the other hand, the combination of both FSH and BMP15 significantly increased glutamine consumption, consistent with increased oxidative metabolism. Hence, the previously reported increases in oocyte developmental competence achieved using combined FSH and BMP15 supplementation likely occurred by equilibrating metabolism within the oocyte rather than shifting the preference for oxidative or reductive metabolism. For example, FSH stimulated glucose metabolism within the cumulus vestment, while BMP15 promoted oxidative phosphorylation through improved mitochondrial function and protection against cellular stress via increased NADPH production. which promotes glutathione recycling.

MATERIALS AND METHODS

Unless stated otherwise, all chemicals were obtained from Sigma–Aldrich (St Louis, MO).

Oocyte Collection and IVM

Cattle ovaries were collected from a local abattoir (T&R, Murray Bridge, South Australia) and transported to the laboratory in warm saline (30–35 °C). Immature COCs were aspirated from ovarian follicles using an 18-gauge needle and a 10-ml syringe, in undiluted follicular fluid. Compact COCs with intact cumulus vestments, at least three somatic-cell layers, and un-granulated ooplasms were selected into undiluted follicular fluid, washed once in maturation medium (bicarbonate-buffered TCM199 (ICN Biochemicals; Irvine, CA) + 0.5 mM pyruvate + 4 mg/ml fatty acid free (FAF) BSA (ICPBio Ltd; Auckland, New Zealand)), and then transferred into the corresponding IVM treatments. The IVM media was supplemented, as indicated, with 100 mIU/ml FSH (Puregon; Organon, Oss, Netherlands) and/or 100 ng/ml BMP15, a concentrated preparation of recombinant human BMP15 pro/mature-

complex produced in our laboratory using 293 T cells, as previously described (Pulkki et al., 2011; Mottershead et al., 2012). Groups of 10 COCs were cultured in 100 μl volumes of pre-equilibrated IVM media, overlaid with paraffin oil (Merck; Darmstadt, Germany), at 38.5 °C in 6% CO_2 in humidified air. Unless otherwise stated, COCs were cultured for 23 hr.

Intra-Oocyte G6PDH Activity Assay

After 21.5 hr of culture ± FSH ± BMP15, COCs were transferred into fresh IVM media containing 23 μM BCB, and cultured for 90 min at 38.5 °C. At the completion of culture, COCs were washed once in wash medium (VitroWash; IVF Vet Solutions, Adelaide, Australia) containing 4 mg/ml fatty-acid-free bovine serum albumin (FAF-BSA). Stained oocytes were assessed using a dissecting microscope. BCB is readily metabolized by G6PDH, hence blue oocytes (BCB^+) arise from COCs with low G6PDH activity and BCB^- oocytes from COCs with high G6PDH activity. Data are presented as the proportion of BCB^- negative (BCB^-) oocytes from the total oocyte pool for each treatment and replicate. Four replicate experiments were performed with 20–30 COCs used within each treatment group and replicate.

Intra-Oocyte IDH Activity and NAD(P)H Levels

Following 23 hr of culture in IVM media without FSH ± 100 ng/ml BMP15, COCs were transferred into VitroWash + 4 mg/ml FAF BSA containing 0 or 1 mM oxalomalate. (A dose response of oxalomalate revealed that media containing 2 mM oxalomalate or higher had high levels of background fluorescence (Supplementary Figure S1), so 1 mM oxalomalate was used in subsequent experiments.) COCs were transferred to 5 μl of corresponding wash medium ± oxalomalate, overlaid with oil in glass-bottom confocal dishes (Cell E&G; Houston, TX). Autofluorescence images were captured of the live oocytes using a FluoView FV10i confocal microscope and accompanying software (Olympus; Tokyo, Japan), measuring FAD with the green (473 nm excitation; 490–590 nm emission) and NADH/NADPH with the blue (405 nm excitation; 420–520 nm emission) filters. Microscope settings, such as laser intensity and image size, were kept constant. Quantification of the fluorescence intensity was determined using ImageJ imaging software (National Institutes of Health, Bethesda, MD), with the raw data normalized to fluorescence beads (InSpeck, Molecular Probes; Eugene, OR). Three replicate experiments were performed with 10 COCs measured per treatment group per replicate.

Intra-Oocyte GSH, Mitochondrial Activity, and ROS Levels

COCs were denuded after 23 hr of culture by repeat pipetting, and then transferred into VitroWash + 4 mg/ml FAF–BSA + 20 μM PF1 for 1 hr; 12.5 μM MCB for 30 min; and 200 nM Mitotracker Red CMXROS (Molecular Probes) for 15 min at 38.5 °C in darkness. Oocytes were washed once in VitroWash + 4 mg/ml FAF BSA, and transferred into 2-μl smears of wash medium in glass-bottom confocal dishes.

PF1 is an aryl boronate probe that fluoresces on reaction with H_2O_2 (Chang et al., 2004). It has higher specificity for H_2O_2 and peroxynitrite over other ROS, unlike commonly used non-specific ROS probes such as 2',7'-dichlorohydrofluorescein diacetate (H_2DCFDA)—which also auto-oxidizes and catalyzes superoxide production, leading to false-positive fluorescence (Murphy et al., 2011). PF1 was prepared using microwave irradiation in place of conventional heating: 3',6'-diiodofluoran (Chang et al., 2004) (89 mg, 0.16 mmol), bis(pinacolato) diboron (160 mg, 0.63 mmol), potassium acetate (141 mg, 0.63 mmol), and Pd(dppf)Cl_2 (14 mg, 0.02 mmol) were pre-dried in vacuo, dissolved in dimetheylformamide (4 ml) under a N_2 atmosphere in a sealed microwave vial fitted with a Teflon cap. The light-brown mixture was reacted in a CEM Discover microwave synthesiser (Matthews, NC) at 80 °C for 2 hr. The solvent was removed under reduced pressure to give a dark brown powder, which was purified by column chromatography and eluted with 4:1 hexane:ethyl acetate to give PF1 as a white solid. (40 mg, 45%); ^{1}HNMR ($CDCl_3$, 300MHz): δ(ppm) 8.03 (1H, m), 7.74 (2H, s), 7.60 (2H, m), 7.43 (2H, dd, $J_1 = 7.8$Hz, $J_2 = 1.1$Hz), 7.06 (1H, m), 6.86 (2H, d, $J = 7.8$Hz), 1.35 (24H, s).

Both MCB and Mitotracker Red CMXROS are commercially available fluorescent probes. MCB fluoresces when bound to low-molecular-weight thiol compounds; its highest affinity is for GSH, which represents 99% of the intracellular fluorescence intensity (Keelan et al., 2001). Mitotracker Red accumulates within mitochondria, depending on membrane potential.

Intra-oocyte fluorescence was captured on a Fluoview FV10i confocal microscope using appropriate filter sets: MCB (358 nm excitation; 461 nm emission), PF1 (496 nm excitation; 519 nm emission) , and Mitotracker Red (578 nm excitation; 598 nm emission). Laser intensity, magnification, and image-capture settings remained constant across replicates.

Image processing and analyses were performed using ImageJ software with the plugin/macro option, which allowed for semi-automated analyses. Macros for image file processing and measurements are included as Supplementary data. Briefly, using Macro 1, individual images representing each fluorescent channel were captured, and then converted from Olympus confocal image files (Olympus image format, oif) into 8-bit gray-scale tiff files. The oocyte was selected as a region of interest (ROI) and the background of the image was excluded. Mean intensity (Macro 2) and selected texture-features analyses (gray-level co-occurrence matrices; Macro 3) of the ROI were performed. Macros 2 and 3 are available from the NIH ImageJ website (http://rsb.info.nih.gov/ij/plugins). Gray-level co-occurrence matrix analysis was applied to determine differences in the localization of fluorescence intensity, e.g. the texture (uniformity/smoothness/roughness) of staining patterns (Haralick et al., 1973; Murata et al., 2001; Cabrera 2006). Angular secondary moment represents the texture of the whole

oocyte; contrast represents the texture of sub-cellular organelles; and correlation represents the intensity differences between pixels. A total of 10 COCs used per treatment.

The relationship between MCB fluorescence and intra-oocyte GSH levels was validated by incubating COCs in buthionine sulphoximine (BSO), an inhibitor of the first stage of glutathione synthesis (gamma-glutamylcysteine-synthetase). Groups of 10 COCs were cultured in VitroMat + 4 mg/ml FAF−BSA + 0.1 IU/ml FSH and 0, 1, 2, 5, and 10 mM BSO. After 23 hr of culture, COCs were incubated with 12.5 μM MCB (as above), and fluorescence intensity was determined within denuded oocytes. Results of the dose response are presented in Supplementary Figure S3. Two replicate experiments were performed, with 10 COCs per replicate.

Gene Expression Within the Oocyte and Cumulus-Cell Vestment

Total RNA from 50 COC-derived oocytes or the cumulus cells from 50 COCs was isolated using Trizol, according to manufacturers instructions (Life Technologies; Mulgrave, Australia). Total RNA was treated with 1 IU DNAse (Life Technologies) at 37 °C for 1 hr, as per manufacturers instructions. First-strand complementary DNA (cDNA) was synthesised using random hexamer primers and Superscript III reverse transcriptase (Life Technologies). Gene primers for real-time reverse-transcriptase PCR were designed against published mRNA sequences from the NCBI Pubmed Database using Primer 3 software (Table 2) and synthesised by Geneworks (Geneworks, Adelaide, Australia). Real-time PCR was performed in triplicate for each sample on a Rotor-Gene™ 6000 (Corbett Life Science; Sydney, Australia). In each reaction, cDNA from 10 ng total RNA, 0.1 μl forward and reverse primers, and 10 μl SYBR ® Green Master Mix (Applied Biosystems; Carlsbad, CA), and water were combined to a final volume of 20 μl. All primers were used at an optimized concentration of 25 mM. PCR conditions were as follows: 50 °C for 2 min, 95 °C for 10 min, followed by 40 cycles of 95 °C for 15 sec and 60 °C for 60 sec. Single-product amplification was confirmed by analysis of disassociation curves and ethidium bromide-stained agarose gel electrophoresis. Controls included the absence of cDNA template or the reverse transcriptase enzyme; each showed no evidence of product amplification or genomic DNA contamination. All gene expression was normalized to an *RPL19* (*L19*) internal loading control that was amplified in parallel for each sample. Results were then expressed as a raw expression value using the $2^{-(\Delta\Delta CT)}$ method.

Amino-Acid Turnover by Intact Cumulus Oocyte Complexes

Groups of 10 COCs were cultured ± FSH ± BMP15. After 19 hr of culture, individual COCs were transferred into 2-μl drops of fresh culture medium and cultured for 4 hr. At the completion of the culture period, the COC was removed, 1 μl of the spent medium was transferred into a 1.7-ml microfuge tube, snap-frozen, freeze-dried, and stored at −80 °C. A replicate drop of media without a COC was cultured simultaneously per treatment condition to account for amino acid concentrations within the media.

Freeze-dried samples were analyzed for amino acid composition using a protocol similar to a previous report (Wale and Gardner, 2012). Amino-acid analysis was undertaken using the derivatization-labeling reagent 6-aminoquinolyl-N-hydroxysuccinimidyl carbamate (Aqc) and a triple-quadrupole mass spectrometer (LC-QqQ-MS), to facilitate the concentrations of co-eluted fractions of a variety of amines to be resolved and quantitated by comparison against a standard calibration curve. A 2.5 mM stock solution of amino acids was prepared containing the following: lysine, histidine, asparagine, arginine, taurine, serine, glutamine, glycine, aspartate, glutamate, threonine, alanine, proline, cysteine, tyrosine, methionine, valine, isoleucine, leucine, phenylalanine, and tryptophan. Calibration standards for these amino acids were then prepared by diluting the stock solution to 150, 100, 50, 25, 10, 5, 1, 0.5, 0.1, 0.05, and 0.01 μM in water using volumetric glassware. Norleucine was used as an internal standard in borate buffer containing the antioxidant ascorbic acid and the reducing agent tris(2-carboxyethyl) phosphine. Each dried-media sample, including a control media sample not used for COC incubation, was resuspended in 10 μl of MilliQ water; 10 μl aliquots of each amino acid

TABLE 2. Gene and Primer List for Real-Time Reverse-Transcriptase PCR

Symbol	Gene name	Role	Primer sequence	Size	Accession
GSS	Glutathione synthetase	Glutathione biosynthesis	(F) 5′-CAGCGTGCCATAGAGAATGA (R) 5′-AATATCCGGGCACTTGACAG	234	NM_001015630.1
GSR	Glutathione reductase	Reduces oxidized glutathione	(F) 5′-TGTCATTGTTGGTGCTGGTT (R) 5′-AGCGTTCTCCAGCTCTTCAG	154	NM_001114190.2
GSTA1	Glutathione S-transferase A1	Reduces oxidized glutathione	(F) 5′-CGTCACTACCGAATGTACCAGAAA (R) 5′-TCAAGCTTAGCTCTGTGGGCTAA	101	BC102540.1
GPX1	Glutathione peroxidase 1	Oxidises glutathione in response to H_2O_2	(F) 5′-GATCCTGAATTGCCTGAAGTACGT (R) 5′-AGAGCGGATGCGCCTTCT	104	NM_174076
GPX4	Glutathione peroxidase 4	Oxidises glutathione in response to H_2O_2	(F) 5′-GCCGCTGGCTATAACGTCAA (R) 5′-CCCTTGGGCTGGACTTTCAT	101	NM_174770.3
RPL19			(F) 5′-TGAGGCCCGCAGGTCTAAG (R) 5′-CTTCCTCCTTGGACAGAGTCT TG	101	BC102223

standard were prepared in parallel. To all standards and samples, 70 μl of borate buffer was then added and mixed by vortexing for 20 sec followed by centrifugation (1 min). To each 80 μl volume, 20 μl of Aqc was added, then the solution was vortexed immediately for 20 sec and warmed on a heating block (Thermomixer, Eppendorf) with shaking (1000 rpm) for 10 min at 55 °C. The final solution was then allowed to cool to ambient temperature before centrifugation (1 min), followed by analysis using an Agilent 1200 LC-system coupled to an Agilent 6420 ESI-QqQ-MS (Santa Clara, CA).

The amino acid concentrations in spent media were normalized against a drop of media that had been cultured without a COC, and consumption/production were calculated as pmol per COC per hour of culture (4 hr). A negative value indicates net depletion/consumption whereas positive values represent production/appearance in the COC media samples. Four experimental replicates were performed, with the spent media from two individual COC cultures collected per treatment group, within replicates.

Statistical Analyses

Differences between treatments were determined using a general linear model, with BMP15 and FSH as main effects—except for the IDH assay, where the main effects were BMP15 and oxalomalate. Differences between individual treatment groups were determined using the Bonferroni post-hoc test. Proportional data was arcsine transformed prior to analysis. All statistical tests were performed using SPSS version 22 statistical software and P values less than 0.05 were considered statistically significant.

ACKNOWLEDGEMENTS

The authors would like to thank SEMEX Pty Ltd Australia for the kind gift of bull semen. This study was funded by National Health and Medical Research Council Australia Project (1008137) and Development (1017484) Grants and a collaborative research grant from Cook Medical (Eight Mile Plains, QLD Australia). The Fluoview FV10i confocal microscope was purchased as part of the Sensing Technologies for Advanced Reproductive Research (STARR) facility, funded by the South Australia's Premier's Science and Research Fund. The authors declare no conflict of interest.

REFERENCES

Albertini DF, Combelles CM, Benecchi E, Carabatsos MJ. 2001. Cellular basis for paracrine regulation of ovarian follicle development. Reproduction 121:647–653.

Alm H, Torner H, Lohrke B, Viergutz T, Ghoneim IM, Kanitz W. 2005. Bovine blastocyst development rate in vitro is influenced by selection of oocytes by brillant cresyl blue staining before IVM as indicator for glucose-6-phosphate dehydrogenase activity. Theriogenology 63:2194–2205.

Alvarenga AV, Pereira WC, Infantosi AF, Azevedo CM. 2007. Complexity curve and grey level co-occurrence matrix in the texture evaluation of breast tumor on ultrasound images. Med Phys 34:379–387.

Bhojwani S, Alm H, Torner H, Kanitz W, Poehland R. 2007. Selection of developmentally competent oocytes through brilliant cresyl blue stain enhances blastocyst development rate after bovine nuclear transfer. Theriogenology 67:341–345.

Buccione R, Schroeder AC, Eppig JJ. 1990a. Interactions between somatic cells and germ cells throughout mammalian oogenesis. Biol Reprod 43:543–547.

Buccione R, Vanderhyden BC, Caron PJ, Eppig JJ. 1990b. FSH-induced expansion of the mouse cumulus oophorus in vitro is dependent upon a specific factor(s) secreted by the oocyte. Dev Biol 138:16–25.

Castellano G, Bonilha L, Li LM, Cendes F. 2004. Texture analysis of medical images. Clin Radiol 59:1061–1069.

Cetica P, Pintos L, Dalvit G, Beconi M. 2003. Involvement of enzymes of amino acid metabolism and tricarboxylic acid cycle in bovine oocyte maturation in vitro. Reproduction 126: 753–763.

Chance B, Schoener B, Oshino R, Itshak F, Nakase Y. 1979. Oxidation-reduction ratio studies of mitochondria in freeze-trapped samples. NADH and flavoprotein fluorescence signals. J Biol Chem 254:4764–4771.

Chang MC, Pralle A, Isacoff EY, Chang CJ. 2004. A selective, cell-permeable optical probe for hydrogen peroxide in living cells. J Am Chem Soc 126:15392–15393.

Crawford JL, McNatty KP. 2012. The ratio of growth differentiation factor 9: Bone morphogenetic protein 15 mRNA expression is tightly co-regulated and differs between species over a wide range of ovulation rates. Mol Cell Endocrinol 348:339–343.

de Matos DG, Furnus CC, Moses DF, Baldassarre H. 1995. Effect of cysteamine on glutathione level and developmental capacity of bovine oocyte matured in vitro. Mol Reprod Dev 42:432–436.

Diaz G, Setzu MD, Zucca A, Isola R, Diana A, Murru R, Sogos V, Gremo F. 1999. Subcellular heterogeneity of mitochondrial membrane potential: Relationship with organelle distribution and intercellular contacts in normal, hypoxic and apoptotic cells. J Cell Sci 112:1077–1084.

Downs SM, Humpherson PG, Leese HJ. 1998. Meiotic induction in cumulus cell-enclosed mouse oocytes: Involvement of the pentose phosphate pathway. Biol Reprod 58:1084–1094.

Dumollard R, Duchen M, Carroll J. 2007a. The role of mitochondrial function in the oocyte and embryo. Curr Top Dev Biol 77:21–49.

Dumollard R, Ward Z, Carroll J, Duchen MR. 2007b. Regulation of redox metabolism in the mouse oocyte and embryo. Development 134:455–465.

Haralick RM, Shanmuga K, Dinstein I. 1973. Textural features for image classification. IEEE Trans Syst Man Cybern Syst 3:610–621.

Hemmings KE, Leese HJ, Picton HM. 2012. Amino acid turnover by bovine oocytes provides an index of oocyte developmental competence in vitro. Biol Reprod 86:165–112.

Hussein TS, Froiland DA, Amato F, Thompson JG, Gilchrist RB. 2005. Oocytes prevent cumulus cell apoptosis by maintaining a morphogenic paracrine gradient of bone morphogenetic proteins. J Cell Sci 118:5257–5268.

Hussein TS, Sutton-McDowall ML, Gilchrist RB, Thompson JG. 2011. Temporal effects of exogenous oocyte-secreted factors on bovine oocyte developmental competence during IVM. Reprod Fertil Dev 23:576–584.

Hussein TS, Thompson JG, Gilchrist RB. 2006. Oocyte-secreted factors enhance oocyte developmental competence. Dev Biol 296:514–521.

Keelan J, Allen NJ, Antcliffe D, Pal S, Duchen MR. 2001. Quantitative imaging of glutathione in hippocampal neurons and glia in culture using monochlorobimane. J Neurosci Res 66:873–884.

Krisher R. 2013. In vivo and in vitro environmental effects on mammalian oocyte quality. Ann Rev Anim Biosci 1:393–417.

Larsen WJ, Wert SE. 1988. Roles of cell junctions in gametogenesis and in early embryonic development. Tissue Cell 20: 809–848.

Li R, Norman RJ, Armstrong DT, Gilchrist RB. 2000. Oocyte-secreted factor(s) determine functional differences between bovine mural granulosa cells and cumulus cells. Biol Reprod 63:839–845.

Losa GA, Castelli C. 2005. Nuclear patterns of human breast cancer cells during apoptosis: Characterisation by fractal dimension and co-occurrence matrix statistics. Cell Tissue Res 322:257–267.

Matoba S, Bender K, Fahey AG, Mamo S, Brennan L, Lonergan P, Fair T. 2014. Predictive value of bovine follicular components as markers of oocyte developmental potential. Reprod Fertil Dev 26:337–345.

Matzuk MM, Burns KH, Viveiros MM, Eppig JJ. 2002. Intercellular communication in the mammalian ovary: Oocytes carry the conversation. Science 296:2178–2180.

Mayevsky A, Chance B. 1982. Intracellular oxidation-reduction state measured in situ by a multichannel fiber-optic surface fluorometer. Science 217:537–540.

Mester B, Ritter LJ, Pitman JL, Bibby AH, Gilchrist RB, McNatty KP, Juengel JL, McIntosh CJ. 2014. Oocyte expression, secretion and somatic cell interaction of mouse bone morphogenetic protein 15 during the peri-ovulatory period. Reprod Fertil Dev. doi:10.107/RD13336

Mittra AK, Parekh R. 2011. Automated detection of skin diseases using texture features. Int J Eng Sci Technol 3:4801–4808.

Mottershead DG, Ritter LJ, Gilchrist RB. 2012. Signalling pathways mediating specific synergistic interactions between GDF9 and BMPI15. Mol Hum Reprod 18:121–128.

Murata S, Herman P, Lakowicz JR. 2001. Texture analysis of fluorescence lifetime images of AT- and GC-rich regions in nuclei. J Histochem Cytochem 49:1443–1451.

Murphy MP, Holmgren A, Larsson NG, Halliwell B, Chang CJ, Kalyanaraman B, Rhee SG, Thornalley PJ, Partridge L, Gems D, Nystrom T, Belousov V, Schumacker PT, Winterbourn CC. 2011. Unraveling the biological roles of reactive oxygen species. Cell Metab 13:361–366.

Pulkki MM, Myllymaa S, Pasternack A, Lun S, Ludlow H, Al-Qahtani A, Korchynskyi O, Groome N, Juengel JL, Kalkkinen N, Laitinen M, Ritvos O, Mottershead DG. 2011. The bioactivity of human bone morphogenetic protein-15 is sensitive to C-terminal modification: Characterization of the purified untagged processed mature region. Mol Cell Endocrinol 332:106–115.

Richani D, Sutton-McDowall ML, Frank LA, Gilchrist RB, Thompson JG. 2014. Effect of epidermal growth factor-like peptides on the metabolism of in vitro- matured mouse oocytes and cumulus cells. Biol Reprod 90:49.

Rieger D, Loskutoff NM. 1994. Changes in the metabolism of glucose, pyruvate, glutamine and glycine during maturation of cattle oocytes in vitro. J Reprod Fertil 100:257–262.

Roca J, Martinez E, Vazquez JM, Lucas X. 1998. Selection of immature pig oocytes for homologous in vitro penetration assays with the brilliant cresyl blue test. Reprod Fertil Dev 10:479–485.

Salhab M, Dhorne-Pollet S, Auclair S, Guyader-Joly C, Brisard D, Dalbies-Tran R, Dupont J, Ponsart C, Mermillod P, Uzbekova S. 2013. In vitro maturation of oocytes alters gene expression and signaling pathways in bovine cumulus cells. Mol Reprod Dev 80:166–182.

Salhab M, Tosca L, Cabau C, Papillier P, Perreau C, Dupont J, Mermillod P, Uzbekova S. 2011. Kinetics of gene expression and signaling in bovine cumulus cells throughout IVM in different mediums in relation to oocyte developmental competence, cumulus apoptosis and progesterone secretion. Theriogenology 75:90–104.

Salustri A, Ulisse S, Yanagishita M, Hascall VC. 1990a. Hyaluronic acid synthesis by mural granulosa cells and cumulus cells in vitro is selectively stimulated by a factor produced by oocytes and by transforming growth factor-beta. J Biol Chem 265: 19517–19523.

Salustri A, Yanagishita M, Hascall VC. 1990b. Mouse oocytes regulate hyaluronic acid synthesis and mucification by FSH-stimulated cumulus cells. Dev Biol 138:26–32.

Sanchez MC, Sedo CA, Julianelli VL, Romanato M, Calvo L, Calvo JC, Fontana VA. 2013. Dermatan sulfate synergizes with heparin in murine sperm chromatin decondensation. Syst Biol Reprod Med 59:82–90.

Schliess F, Hoehme S, Henkel SG, Ghallab A, Driesch D, Bottger J, Guthke R, Pfaff M, Hengstler JG, Gebhardt R,

Haussinger D, Drasdo D, Zellmer S. 2014. Integrated metabolic spatial-temporal model for the prediction of ammonia detoxification during liver damage and regeneration. Hepatology 60:2040–2051.

Skala M, Ramanujam N. 2010. Multiphoton redox ratio imaging for metabolic monitoring in vivo. Methods Mol Biol 594:155–162.

Steeves TE, Gardner DK. 1999. Metabolism of glucose, pyruvate, and glutamine during the maturation of oocytes derived from pre-pubertal and adult cows. Mol Reprod Dev 54:92–101.

Su YQ, Wu X, O'Brien MJ, Pendola FL, Denegre JN, Matzuk MM, Eppig JJ. 2004. Synergistic roles of BMP15 and GDF9 in the development and function of the oocyte-cumulus cell complex in mice: Genetic evidence for an oocyte-granulosa cell regulatory loop. Dev Biol 276:64–73.

Sudiman J, Ritter LJ, Feil DK, Wang X, Chan K, Mottershead DG, Robertson DM, Thompson JG, Gilchrist RB. 2014. Effects of differing oocyte-secreted factors during mouse in vitro maturation on subsequent embryo and fetal development. J Assist Reprod Genet 31:295–306.

Sugimura S, Ritter LJ, Sutton-McDowall ML, Mottershead DG, Thompson JG, Gilchrist RB. 2014. Amphiregulin co-operates with bone morphogenetic protein 15 to increase bovine oocyte developmental competence: Effects on gap junction-mediated metabolite supply. Mol Hum Reprod 20: 499–513.

Sutton ML, Cetica PD, Beconi MT, Kind KL, Gilchrist RB, Thompson JG. 2003a. Influence of oocyte-secreted factors and culture duration on the metabolic activity of bovine cumulus cell complexes. Reproduction 126:27–34.

Sutton ML, Gilchrist RB, Thompson JG. 2003b. Effects of in-vivo and in-vitro environments on the metabolism of the cumulus-oocyte complex and its influence on oocyte developmental capacity. Hum Reprod Update 9:35–48.

Sutton-McDowall M, Gilchrist R, Thompson J. 2010. The pivotal role of glucose metabolism in determining oocyte developmental competence. Reproduction 139:685–695.

Sutton-McDowall ML, Mottershead DG, Gardner DK, Gilchrist RB, Thompson JG. 2012. Metabolic differences in bovine cumulus-oocyte complexes matured in vitro in the presence or absence of follicle-stimulating hormone and bone morphogenetic protein 15. Biol Reprod 87:87–88.

Takahashi M, Nagai T, Hamano S, Kuwayama M, Okamura N, Okano A. 1993. Effect of thiol compounds on in vitro development and intracellular glutathione content of bovine embryos. Biol Reprod 49:228–232.

Urner F, Sakkas D. 2005. Involvement of the pentose phosphate pathway and redox regulation in fertilization in the mouse. Mol Reprod Dev 70:494–503.

Van Blerkom J. 2009. Mitochondria in early mammalian development. Semin Cell Dev Biol 20:354–364.

Vanderhyden BC, Macdonald EA. 1998. Mouse oocytes regulate granulosa cell steroidogenesis throughout follicular development. Biol Reprod 59:1296–1301.

Varone A, Xylas J, Quinn KP, Pouli D, Sridharan G, McLaughlin-Drubin ME, Alonzo C, Lee K, Munger K, Georgakoudi I. 2014. Endogenous two-photon fluorescence imaging elucidates metabolic changes related to enhanced glycolysis and glutamine consumption in pre-cancerous epithelial tissues. Cancer Res 74:3067–3075.

Wale PL, Gardner DK. 2012. Oxygen regulates amino acid turnover and carbohydrate uptake during the preimplantation period of mouse embryo development. Biol Reprod 87:24–28.

Yeo CX, Gilchrist RB, Thompson JG, Lane M. 2008. Exogenous growth differentiation factor 9 in oocyte maturation media enhances subsequent embryo development and fetal viability in mice. Hum Reprod 23:67–73.

Supporting Information

Additional supporting information may be found in the online version of this article at the publishers web-site.

MRD